Thermally Induced Stresses in Glazing Systems

PIOTR TOFILO AND MICHAEL DELICHATSIOS*
Fire Safety Engineering Research and Technology Center (FireSERT), University of Ulster, Jordanstown BT37 0QG, UK

ABSTRACT: A thorough examination has been performed of the thermally induced stresses on a window in an enclosure-fire environment. Analytical and numerical methods establish the importance of bridling stress (due to axial elongation) and flexing stress (due to normal deformation). Most previous studies omitted the consideration of flexing stresses. Maximum stresses, being the sum of bridling and flexing stresses on the side, have been calculated for varying aspect ratios of a rectangular window and for varying ratios of shaded width to the window sides. For uniform width and heating (e.g., represented, by constant high temperature in the heated region and ambient temperature in the shaded region), the maximum stresses are bridling and equal to those of an infinite strip shaded on two sides when the shaded width is less than 40% of the short side. For nonuniform shading (e.g., due to radiation blockage) or nonuniform heating, flexing stresses contribute to the total stress by an increase up to 50%. These new results have been applied in predicting the magnitude of stresses and the location of the first crack in well-controlled experiments and measurements. These results are important because they extend and delineate the limitations of currently used relations for determining thermally induced stresses and times of first cracking in windows.

KEY WORDS: glass breakage, flexing stress, bridling stress, enclosure fire, thermal stress.

INTRODUCTION

CRACKING AND SUBSEQUENT fallout of glazing can change dramatically the fire intensity in enclosure fires by generating, for example, an additional opening feeding fresh combustion air into the fire or assisting the venting of the gases if such cracking and fallout occurs in the upper part of a glazing panel covering the wall of an enclosure. Thermal expansion of the

*Author to whom correspondence should be addressed. E-mail: m.delichatsios@ulster.ac.uk

1042-3915/10/02 0101–16 $10.00/0 DOI: 10.1177/1042391509344243

SAGE Publications, Los Angeles, London, New Delhi and Singapore

glazing caused by heat fluxes from the fire produces stresses of sufficient magnitude to initiate cracks in the glazing. The relation between the stresses and the temperature distribution on the glazing enables the prediction of times to first crack and subsequent cracks. Old and recent work [1–5] suggests that this relationship is simple:

$$\varepsilon_b = \sigma_b / E = \beta \Delta T_b \tag{1}$$

Equation (1) represents the thermally induced strain at the edge of the glass at the breaking point. The first part of this equation is Hooke's law and the second is the definition of the thermal coefficient of linear expansion, $\beta = (\mathrm{d}l/\mathrm{d}T)/l$. Using typical values for the glass breaking stress [1], $10 < \sigma_b < 50$ MPa, and Young's modulus, $E = \sim 72$ GPa, in Hooke's law gives small breaking strains, $1.5 \times 10^{-4} < \varepsilon_\mathrm{b} < 7 \times 10^{-4}$; that is, 0.015–0.07% thermal expansion suffices to break the glass. Note that the frame offers no restraint to the glass since the maximum thermal expansion, <1 mm, is less than the normal gap of several millimeter between the frame and the pane [3,4]. From Equation (1), assuming $\beta = \sim 9 \times 10^{-6}\,\mathrm{K}^{-1}$, the spatially averaged glass temperature rise at breaking is $20^\circ\mathrm{C} < \Delta T_g < 80^\circ\mathrm{C}$. The spatially averaged glass temperature is defined through Figure 1 taken from [3], where the coordinate origin is placed at the inner edge of the shaded region of width s; z is into the glass with zero on the fire side and the glass thickness is L so that $0 \le z \le L$; y is toward the center of the pane and z is along the edge of the shaded region.

It has been claimed [3,4] that 'the greatest simplification comes from recognizing that it is the difference between the integrated bulk temperature over the central pane and the coldest temperature on the pane edge which

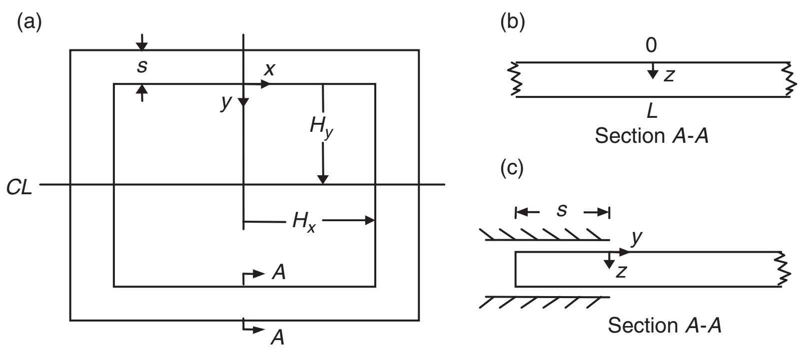

Figure 1. *Window geometry: z is the depth, y is normal to the shaded region, x is along the shading, s is the width of the shading, H_y and H_x are the exposed pane half-lengths and L is the glass thickness. Reproduced with kind permission by the International Association for Fire Safety Science [3].*

produces the strain' that leads to cracking, allowing Keski-Rahkonen to write that 'the maximum stresses are located at cold spots [1,2].' The point of crack origin will be the edge cold spot with the largest stress-concentrating defect. Based on these analyses [3] the temperature difference ΔT_b in Equation (1) is:

$$DT_b = \overline{T}_{exposed} - T_{coldest}, \tag{2}$$

Where

$$\overline{T}_{exposed} \equiv \int_0^L \int_0^{H_y} \int_0^{H_x} \frac{T(x, y, z, t_b)}{L\ H_y\ H_x} \mathrm{d}x\mathrm{d}y\mathrm{d}z, \tag{3}$$

with the upper right quadrant assumed to represent the whole pane.

The relation defined by Equations (1)–(3) proposes that the thermal strain and stresses are independent of (a) the detailed temperature distribution, and (b) the aspect ratio or shape of the window. Examination, however, of earlier work on thermal expansion of glazing in solar energy applications [6–8] and theoretical analysis show that this conclusion and claim needs revisiting, which this article presents. It is worth noticing that the more recent fire related theoretical work [1–4] has not included references to those earlier papers which were related to heating of windows by solar radiation [7,9]. Additional experimental research (e.g., [5]) following the theoretical work in [1–4,6,7] was not able to definitely validate or challenge Equation (1). In fact, it was found that Equation (1) is not appropriate for fitting the experimental results without introducing a proportionality parameter, f (ranging from 0.2 to 0.8).

THERMAL STRESS: ANALYTIC SOLUTIONS

Dimensional analysis and numerical simulation show that variations of stresses and temperature in depth can be neglected because the glazing thickness is much smaller than the other dimensions. Therefore, the development of stresses and the temperature distribution are 2D so that the glazing behaves as a thin plate. This is an approximation all previous investigators have made [1–4,6–9] including in the analytic solutions of Keski-Rahkonen [1,2] which are discussed in detail next. These solutions, adopted by Pagni [3,4,6], are represented by Equations (1) and (2).

Keski-Rahkonen [1,2] examined two geometries, a long rectangular strip [1] and a circular glass plane having a radially symmetric temperature distribution [2]. The solution for the circular glass pane found in standard texts [10] shows that Equation (1) can indeed express the thermal stress, where the average temperature of the circular pane having radius, a, is:

$$\overline{T}_{exposed} = \frac{1}{\pi a^2} \int_0^a 2\pi T r \mathrm{d}r \tag{4}$$

A more complete solution for the long strip than those considered in [1] and in [3,4,6] is developed in the next section.

The Complete Solution for a Long Strip of Glazing

The investigation of thermal stresses will compare the complete solution with the solution of Keski-Rahkonen [1,3].

For quick reference, the complete stress equations for a rectangular thin plate and their boundary conditions are recast in the Appendix [10]. For glazing applications, the edges, having space to expand (Figure 1(c)), are traction free, which means that stresses normal to the edge are zero at each edge. A rectangular window ABCD of size ($2b \times 2c$) is shown in Figure 2 having a x–y coordinate system with origin at the center of the window. For aspect ratios $b/c > 3$, numerical solutions [8,11–13] show that the window behaves as an infinitely long strip.

Similar to [1,3], a temperature distribution which is function only of y: $T = T(y)$ is considered. The traction free boundary conditions are (see Appendix):

On sides AD and BC: normal and shear stresses are zero

$$\sigma_{xx} = \sigma_{yx} = 0, \tag{5a}$$

but the normal y-stress (called flexing [8] due to deformation) is not:

$$\sigma_{yy} \neq 0. \tag{5b}$$

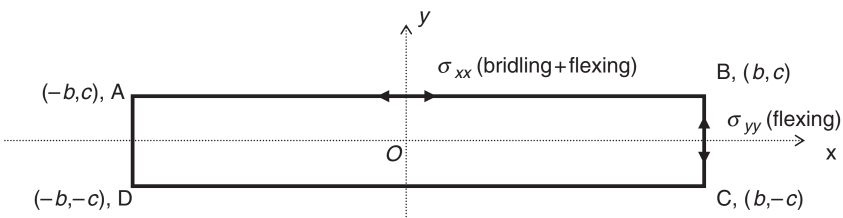

Figure 2. A rectangular window in the form of a long strip.

On sides AB and DC: similarly, normal and shear stresses are zero

$$\sigma_{xy} = \sigma_{yy} = 0, \tag{5c}$$

but the normal x-stress is not:

$$\sigma_{xx} \neq 0. \tag{5d}$$

This stress is the sum of so called *bridling stress* [8], due to axial tension, and flexing stress due to deformation. In addition, near the center, $x = 0$ of the strip, the y stresses are zero, $\sigma_{xy} = \sigma_{yy} = 0$ and the remaining parameters are functions only of y near the center of the strip. But still the y normal stress is different from zero $\sigma_{yy} \neq 0$ on the lateral sides AD and BC as also verified later by the numerical solution in the next section. For the conditions near the y-axis, the compatibility relation for the stresses (see Equation (A6)) gives:

$$\frac{\partial^2 \varepsilon_{xx}}{\partial y^2} = 0 \tag{6a}$$

The x normal stress near the center axis Oy (Figure 2) is given by Equation (A5a),

$$\frac{1}{E}\sigma_{xx} = \varepsilon_{xx} - \beta T \tag{6b}$$

The solution of the system of Equations 5 and 6 is simply:

$$\varepsilon_{xx} = Ay + B, \tag{7a}$$

$$\frac{1}{E}\sigma_{xx} = Ay + B - \beta T, \tag{7b}$$

where the constants A and B need two boundary conditions to be derived. These boundary conditions are related to the boundary conditions for the normal x stress on sides AD and BC:

$$\int_{-c}^{+c} \sigma_{xx} \mathrm{d}y = 0, \tag{8a}$$

$$\int_{-c}^{+c} y\sigma_{xx} \mathrm{d}y = 0, \tag{8b}$$

The latter condition, not considered in [1,3] is necessary when the temperature field is not symmetric in the y-direction. Using Equations (8a) and (8b) together with Equation (7b), provides the coefficients A and B and hence, the stress and the strain:

$$A = \frac{3\beta}{2c^3} \int_{-c}^{+c} yT\mathrm{d}y, \tag{8c}$$

$$B = \beta \int_{-c}^{+c} \frac{T}{2c}\mathrm{d}y, \tag{8d}$$

$$\frac{1}{E}\sigma_{xx} = \frac{3\beta}{2c^3} y \int_{-c}^{+c} yT\mathrm{d}y + \beta \int_{-c}^{+c} \frac{T\mathrm{d}y}{2c} - \beta T = \frac{3\beta}{2c^3} y \int_{-c}^{+c} yT\mathrm{d}y + \beta(T_{av} - T), \tag{8e}$$

$$\varepsilon_{xx} = Ay + B = y\frac{3\beta}{2c^3} \int_{-c}^{+c} yT\mathrm{d}y + \beta \int_{-c}^{+c} \frac{T}{2c}\mathrm{d}y, \tag{8f}$$

where the average temperature in the strip is:

$$T_{av} = \int_{-c}^{+c} \frac{T}{2c}\mathrm{d}y. \tag{8g}$$

For a temperature variation *symmetric in y*, the coefficient $A = 0$ and the x normal stress is:

$$\frac{1}{E}\sigma_{xx} = \beta \int_{-c}^{+c} \frac{T}{2c}\mathrm{d}y - \beta T = \beta(T_{av} - T). \tag{9a}$$

The stress is tension at the edges and contraction near at the center of the strip. The strain being independent of y is equal to:

$$\varepsilon_{xx} = \beta T + \frac{1}{E}\sigma_{xx} = \beta T_{av} \tag{9b}$$

The latter result means that there is no deformation of the long strip near its center ($x = 0$) along the y-axis. The normal stresses caused by expansion, but without deformation in the x direction, are called bridling stresses [8].

For an *asymmetric* distribution of temperature A is not zero, the strain (see Equation (8f)) is a function of y and the strip sustains deformation in the y-direction so that the stress σ_{xx} is the sum of a flexing $((3\beta/2c^3)y\int_{-c}^{+c} yT\mathrm{d}y)$ and a bridling component $(\beta(T_{av} - T))$.

Equation (9a) is the same as the result given by Keski-Rahkonen [1], also adopted by Pagni [3] which shows that the aforementioned results are only valid for a temperature distribution even in the y-direction. In addition, the previous derivations [1,3] imply that the y normal stress is everywhere zero on the sides BC and AD, a result that is not supported by [7] and by numerical solutions in the next section. It is important to note that the y stresses caused on the sides BC and AD are due to flexing and deformation by expansion. These stresses are called flexing stresses. It is concluded that Equation (1) for the stress (where Equation (2) defines the temperature) is not generally valid and does not include the flexing stresses, which will be shown to have a significant contribution to the cracking of a glazing system.

Numerical analysis is applied to determine the influence of the temperature distribution, aspect ratio and shaded area on the stresses. To focus the present investigation on the stresses, the discussion of the thermal field is bypassed by considering the temperature to be constant in the exposed area and equal to zero in the shaded area (detailed discussion of the temperature field for an applied heat flux is available in [14]). The shaded area is taken to have the same width all around the window (Figure 3(a)) or different widths in the vertical direction (Figure 3(b)). The chosen representation of the temperature field in Figure 3(a) is applicable for a window in the hot layer in an enclosure and for times prior to a temperature increase by diffusion at the outer cold edges of the glazing. The situation of variable vertical shaded area in Figure 3(b) represents an anticipated vertical variation of the heat fluxes from a fire in an enclosure when the window extends over the height of the enclosure from the hot to the cold layer, again for times prior to a temperature increase by diffusion at the outer cold edges of the glazing.

NUMERICAL INVESTIGATION OF THERMAL STRESSES

The numerical investigation has been carried out using three different finite element computer codes [11–13] for comparison and verification of the results. Moreover, an earlier numerical solution by NASA based on a collocation method [8] was also consulted for validating the numerical results. The numerical results agreed with the exact solution for the infinite

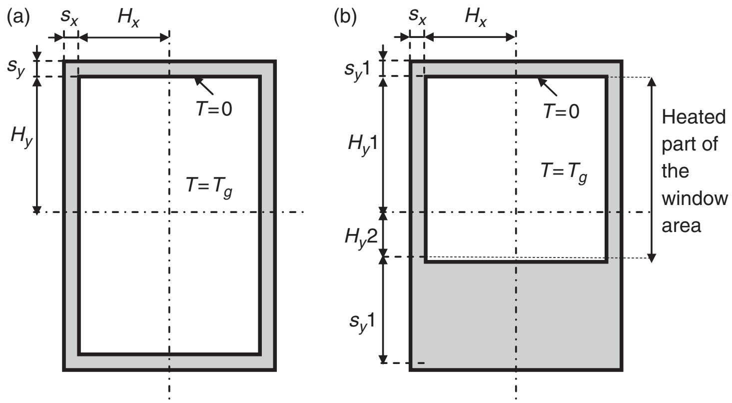

Figure 3. *A window heated with a shaded region of constant width representing a window located: (a) totally in the hot layer, and (b) partially in the hot and cold layers of an enclosure fire.*

strip (e.g., Equations (9a) and (9b)). Numerous calculations for the stresses were carried out to elucidate the physics [14] but results are only discussed here for the conditions of Figure 3(a) and (b), which represent realistic distributions of temperatures near the shaded region [14].

From the linearity of the stress equation (see Appendix) and computer calculations, all configurations in Figure 3(a) and (b) have been found to be representable by multiple superposition of the solutions for a single strip shading (Figure 4(a)) and a corner shading (Figure 4(b)).

For these two cases the stress tensor in any location can be expressed in terms of the following relations:

$$\frac{\sigma_{ij}(x,y)}{E\beta T_G} = \text{function}\left(\frac{s_y}{H_y}, \frac{H_x}{H_y}\right) \text{ for the single strip shading,} \tag{10a}$$

$$\frac{\sigma_{ij}(x,y)}{E\beta T_G} = \text{function}\left(\frac{s_x}{S_y}, \frac{s_y}{H_y}, \frac{H_x}{H_y}\right) \text{ for the corner configuration.} \tag{10b}$$

For calculating the breakage time, the maximum stresses (set equal to the yield stress) are needed at the edges; these stresses occur at the center of a side edge or at the edge junction of the large cold shaded area with the hot part of the window, that is, at a point having coordinates (s_x, $s_{y1}, +H_{y1}+H_{y2}$) in Figure 3(b). The generalized functions in Equations (10a) and (10b) can be obtained by using response surface functions derived from the numerical results. In this article, representative cases for the configurations in Figure 3(a) and (b) are presented to effect modifications of

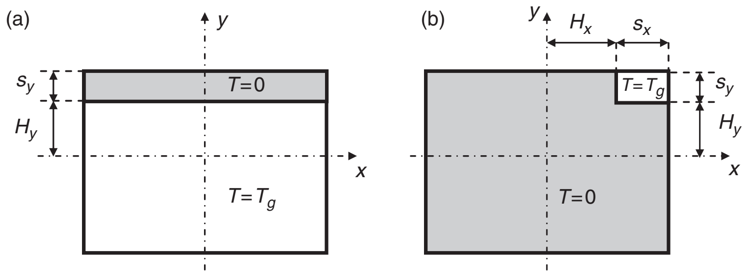

Figure 4. *Basic geometries for multiple superposition: (a) single strip shaded, and (b) everything but corner region shaded.*

Equations (1) and (2) and provide simple, useful results discussed in the next section. The following discussion shows the significance of the flexing stresses and demonstrates that stresses higher than the ones calculated form Equations (1) and (2) could arise.

Stresses in a Window with Constant Width of the Shaded Area

The stresses and temperature fields can be deduced from the superposition of two strip configurations (horizontal and vertical), a corner configuration and a uniform temperature configuration (no stress) as shown in Figure 5. All cases of aspect ratio and shaded width fraction (s_y/H_y) have been examined in [14]. Here, only the stresses for a square window (i.e., $H_x/H_y = 1$) are presented utilizing the superposition shown in Figure 5.

It has been found that for shaded widths $s_y/H_y < 0.4$, the corner configuration does not significantly contribute to the maximum stresses in the center of the edges even though it prevents the distortion of the plate near the edges [14]. The bridling and flexing stresses for the strip configuration of all aspect and width ratios are plotted in Figure 6(a) and the stresses for the square window are shown in Figure 6(b). All stresses are normalized by the stress, σ_∞, (derived from Equation (9a)) at the center of the top edge for an infinite strip having a shaded width, s_y on both sides:

$$\sigma_\infty = \beta E T_g/(1 + s_y/H_y) \tag{11}$$

In deriving Equation (11), the temperature in the shaded area is denoted as zero.

The following remarks can be made regarding Figure 6(a) and (b):

(1) Both bridling and flexing stresses for the strip configuration shaded on two opposite sides are less than the maximum value for an infinite strip (Figure 6(a)). Such an arrangement of glazing having a shaded area only on two opposite sides can be considered as a modification of current

installation methods to reduce the maximum stresses and hence, the propensity of windows to break.

(2) The stresses at the center of the edges for the square window with constant shaded width are nearly equal to stresses for an infinite strip (Figure 6(b)) for widths $s_y/H_y < 0.4$. This behavior may be explained by the observation that these stresses are basically bridling stresses because

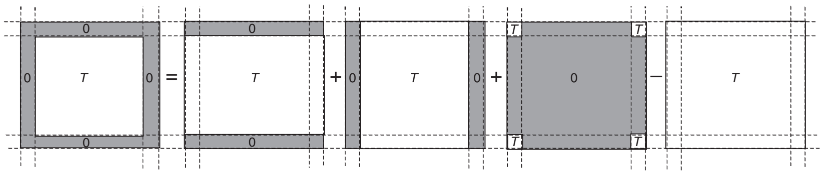

Figure 5. *Superposition of simple configurations to represent a window with constant width of the shaded area.*

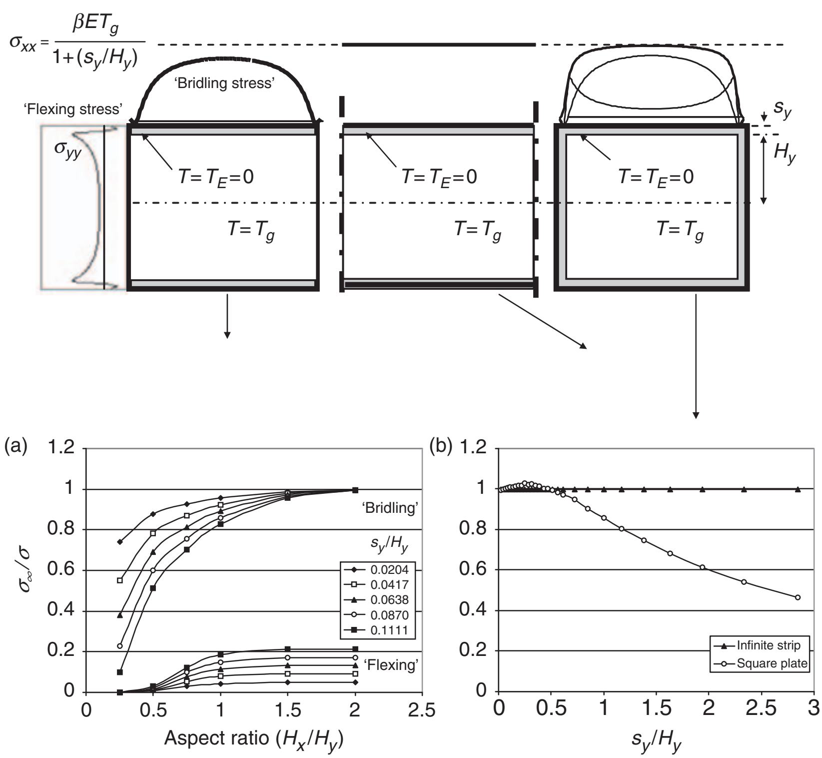

Figure 6. *Stresses at the center of the sides normalized by the bridling stress of an infinite strip (Equation (11)): (a) for a strip of variable aspect ratio; (b) for a square window and variable shaded width ratio. The diagrams above the figures indicate the magnitudes of the superimposing stresses.*

the corner configuration in Figure 6(a) restricts the deformation of the edges. For larger widths $s_y/H_y > 0.4$ the stresses are reduced and have been shown to be proportional to the fraction of the area heated [14].

From the exhaustive work in [14], it has been found that the stresses for a window of *any aspect ratio* with constant shaded width are given by the relation for the infinite strip as in Equation (11) if $s_y/H_y < 0.4$. The maximum stresses for both sides are the same and their magnitude depends on the maximum width ratio s_y/H_y or s_x/H_x to be used in Equation (11).

Stresses in a Window with Nonuniform Heating or Variable Width of the Shaded Area in the Vertical Direction

As discussed in the previous section, the stresses and temperature fields can be deduced from the superposition of simpler strip configurations as shown in Figure 7(a). We restrict the presentation here for a square window. Because the temperature field is asymmetric, flexing, and bridling stresses are important for the vertical and horizontal sides both in the strip and the window configurations. The stresses are normalized by the maximum stress using Equation (11) for an infinite two-sided strip having a shaded width equal to the smaller width in Figure 7(a). The maximum stresses on the

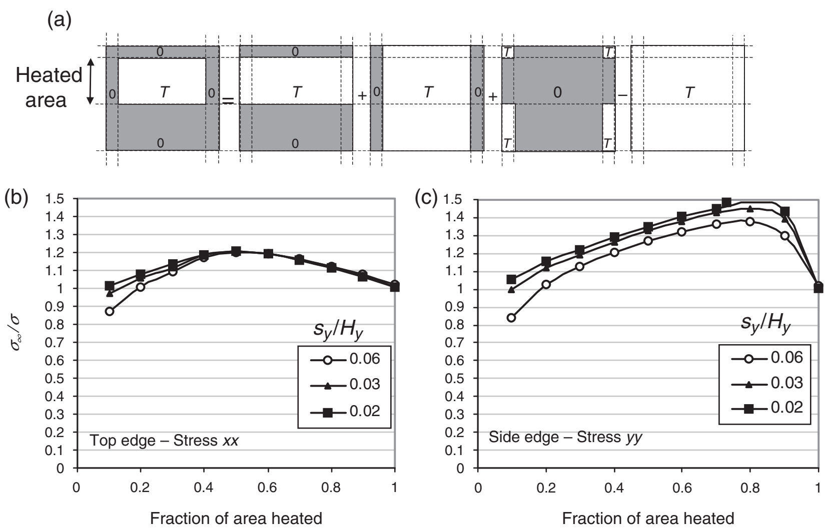

Figure 7. *(a) Superposition of simpler configurations to represent the temperature and stress in a window with nonuniform heating, (b) top edge, and (c) side edge stresses normalized by the bridling stress in an infinite strip (Equation (11)) for variable shaded width (s_y/H_y) and fraction of area heated.*

horizontal and vertical sides are plotted in Figure 7(b) and (c) against the fraction of the area heated as defined in Figure 7(a).

The results shown in Figures 7(b)–(d) show that:

(1) The stresses are higher on the vertical side and about 50% more than the stress for uniform width and temperature. This is applies to all aspect ratios [14].

(2) Both bridling and flexing stresses contribute to the total stress.

OUTLINE OF COMPARISONS WITH EXPERIMENTS

Experiments [14] in enclosure fires have validated the previous analysis which also provided an explanation of why cracking occurs on the vertical side in these experiments (Figure 8(a)–(c)). Briefly, Figure 8(a) and (b)

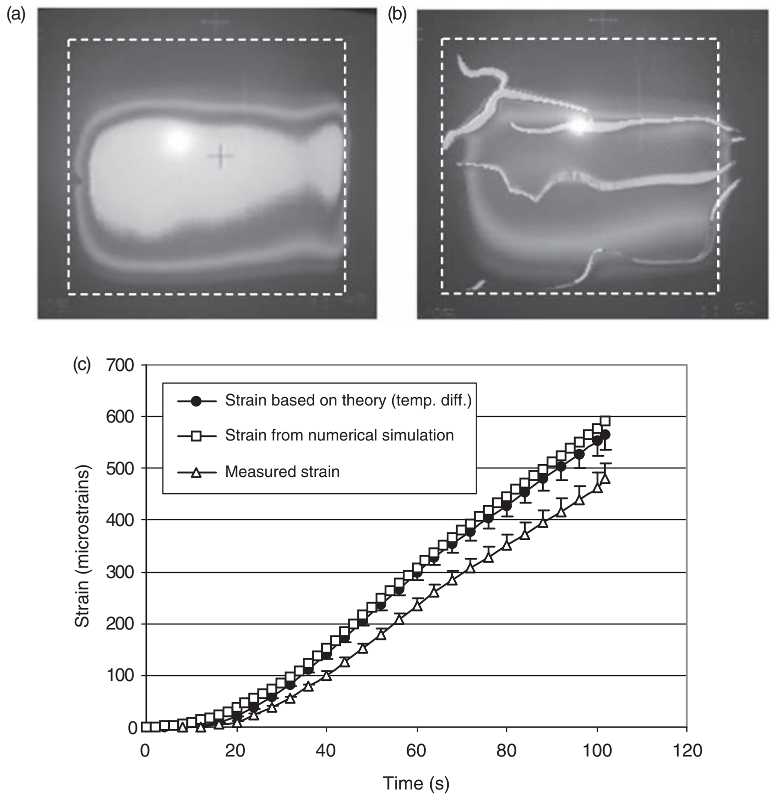

__Figure 8.__ (a,b) Temperature distribution before cracking and cracking patterns on glazing, (c) Comparison of measured and calculated strains in a glazing experiment (uniform heat flux experimentally measured was used over all the window exposed area for simple calculation and numerical simulation).

illustrate the temperature profile and the cracking patterns on a window obtained by an infrared camera whereas Figure 8(c) provides a comparison of predicted with measured values of the strains. The first crack occurred on the vertical sides where the maximum stresses are expected (compare with Figure 7(b) and (c)), because significant shading (owing to radiation blockage because the window was located at the outside of the wall) was observed in the measurements of temperature distribution as shown in Figure 8(a).

CONCLUSIONS

The analytical equations and numerical calculations developed in this article can be used to determine the dominant mechanisms governing the experimental and measured stress magnitudes and the first crack locations. Major conclusions are:

(1) Analytical and numerical solutions demonstrate the significance of the bridling and flexing stresses in calculating the maximum thermal stresses on a window in a enclosure fire environment (see Equation (8e)).
(2) For nonuniform heating or variable shaded width, the stresses increase by 50% owing to the contribution of flexing stresses added to the bridling stresses (Figure 7(b) and (c)).
(3) For uniform heating and equal shaded width of a rectangular window, the maximum stresses being bridling on both sides are the same and equal to those of an infinite strip corresponding to the long side (for a shaded width less than 40% of the short side; see Figure 6(b)).
(4) These results were applied to predict the stresses, the breaking time and possible first crack location in controlled experiments and measurements of heat fluxes and strains (see Figure 8(c) or [14] for more details).

NOMENCLATURE

E	= Young's modulus (GPa)
H_x, H_y	= Exposed pane half lengths (m)
L	= Glazing thickness (m)
s_x, s_y	= Widths of shaded area (m, see Figure 3)
$\overline{T}_{exposed}$	= Spatially averaged gas temperature (°C)
T_g	= Glazing temperature (°C)
T_E	= Shaded edge temperature (°C)
x, y, z	= Coordinates (m; see Figure 1)

Greek

β	= Thermal expansion coefficient (1/°C)
ΔT_b	= Glass temperature rise at breaking (°C)
ε_{xx}, ε_{yy}, ε_{xy}	= Normal and shear strains
ε_b	= Strain at cracking ($d\ell/\ell$)
σ	= Stress (MPa)
σ_b	= Stress at cracking (MPa)
σ_{xx}, σ_{xy}, σ_{yy}	= Normal and shear stresses (MPa; see Figure 2)
σ_∞	= Maximum stress for an infinite strip (MPa)

APPENDIX: 2D FORMULATION OF STRESSES FOR THIN PLATES

The stress equations in orthogonal co-ordinates are, first, a compatibility equation [10]:

$$\left(\frac{\partial^2}{\partial x^2}+\frac{\partial^2}{\partial y^2}\right)(\sigma_{xx}+\sigma_{yy})+E\alpha\left(\frac{\partial^2}{\partial x^2}+\frac{\partial^2}{\partial y^2}\right)T(x,y)=0, \tag{A1}$$

and then, force equilibrium with no external forces,

$$\frac{\partial\sigma_{xx}}{\partial x}+\frac{\partial\sigma_{xy}}{\partial y}=0,\ \text{and}\ \frac{\partial\sigma_{yy}}{\partial y}+\frac{\partial\sigma_{yx}}{\partial x}=0. \tag{A2}$$

The boundary relations at the edges are for traction free conditions:

$$\sigma_{xx}n_x+\sigma_{xy}n_y=0, \tag{A3}$$

and

$$\sigma_{yx}n_x+\sigma_{yy}n_y=0, \tag{A4}$$

These relations mean that at the window side normal to the x-axis $\sigma_{xx}=\sigma_{yx}=0$ and at the window side normal to the y-axis, $\sigma_{xy}=\sigma_{yy}=0$. The plane strains are related to the stresses by the following equations:

$$\varepsilon_{xx}=\frac{1}{E}(\sigma_{xx}-\nu\sigma_{yy})+\beta T, \tag{A5a}$$

$$\varepsilon_{yy}=\frac{1}{E}(\sigma_{yy}-\nu\sigma_{xx})+\beta T, \tag{A5b}$$

$$\varepsilon_{xy} = 2\frac{E}{1+\nu}\sigma_{xy}. \tag{A5c}$$

Finally, there is strain in the direction z normal to the surface:

$$\varepsilon_{zz} = -\frac{\nu}{E}(\sigma_{xx} + \sigma_{yy}) + \beta T. \tag{A5d}$$

Compatibility, Equation (A1), takes the following form in terms of the strains:

$$\frac{\partial^2 \varepsilon_{yy}}{\partial x^2} + \frac{\partial^2 \varepsilon_{xx}}{\partial y^2} = \frac{2\partial^2 \varepsilon_{xy}}{\partial x \partial y}. \tag{A6}$$

Equation (A1) becomes formally simpler and Equation (A2) is not needed by introducing the Airy stress function $F(x,y)$ which is related to stresses by:

$$\sigma_{xx} = \frac{\partial^2 F}{\partial y^2}, \quad \sigma_{yy} = \frac{\partial^2 F}{\partial x^2}, \quad \sigma_{xy} = -\frac{\partial^2 F}{\partial x \partial y} \tag{A7}$$

These equations have been solved numerically in this work but simple graphical solutions have also been developed, for example in [8].

REFERENCES

1. Keski-Rahkonen, O., "Breaking of Window Glass Close to Fire," *Fire Mater*., Vol. 12, 1988, pp. 61–69.
2. Keski-Rahkonen, O., "Breaking of Window Glass Close to Fire, II: Circular Panes," *Fire Mater*., Vol. 15, 1991, pp. 11–16.
3. Pagni, P.J., "Thermal Glass Breakage-Emmons Invited Plenary Lecture," In: Evans, D.D., ed., *Fire Safety Science – Proceedings of the Seventh Symposium*, International Association for Fire Safety Science, London, 2002.
4. Joshi, A.A. and Pagni, P.J., "Fire-Induced Thermal Fields in Window Glass. I – Theory," *Fire Safety J*., Vol. 22, No. 1, 1994, pp. 25–43.
5. Harada, K., Enomoto, A., Uede, K., and Wakamatsu, T., "Experimental Study on Glass Cracking and Fallout by Radiant Heat Exposure," In: Curtat, M., ed., *Fire Safety Science – Proceedings of the Sixth International Symposium*, International Association for Fire Safety Science, London, 2000, pp 1063–1074.
6. Joshi, A.A. and Pagni, P.J., "Fire-Induced Thermal Fields in Window Glass. II – Experiments," *Fire Safety J*., Vol. 22, No. 1, 1994, pp. 45–65.
7. Mai, Y.W. and Jacob, L.J.S., *Thermal Fracture of Building Glass Subjected to Solar Radiation*, Cambridge, England, ICM 3, 1979, Vol. 3.
8. Roberts, E., Elastic Design Charts for Thin Plates with Span-wise and Chord-wise Variations of Temperature, Technical Note D-1182, National Aeronautics and Space Administration, Washington, DC, 1962.

9. Colvin, J.B. and Lightfoot, D.G., Thermal Stress in Non-rectangular Glazing. Report No. 382, Technical Sales Laboratory, Pilkington, 1974.
10. Landau, L.D. and Lifshitz, E.M., Theory of Elasticity, 2nd edn, Pergamon Press, Oxford,1981, p. 22.
11. Ansys, *Ansys Technical Documentation*, Ansys, Inc., Canonsburg, PA, USA, 2008.
12. Nwosu, D., Kodur, V., Franssen, J.-M. and Hum, J., User Manual for SAFIR, A Computer Program for Analysis of Structures at Elevated Temperature Conditions. Internal Report 782, National Research Council of Canada, Ottawa, Oct. 1999.
13. FireCrack Technical Documentation. FireSERT Internal report, University of Ulster, Jordanstown, UK, 2008.
14. Tofilo, P., ''Factors Controlling the Behaviour of Glazing in Enclosure Fires'', PhD Thesis, University of Ulster, Jordanstown, UK, 2006.